

Rapid Commun. Mass Spectrom. 2013, 27, 1237–1250
(wileyonlinelibrary.com) DOI: 10.1002/rcm.6575

Investigation of Galaxolide degradation products generated under oxidative and irradiation processes by liquid chromatography/hybrid quadrupole time-of-flight mass spectrometry and comprehensive two-dimensional gas chromatography/time-of-flight mass spectrometry

S. Herrera López^{1,4}, M. D. Hernando², M. J. Gómez^{1,4}, J. Santiago-Morales³, R. Rosal^{1,3} and A. R. Fernández-Alba^{1,4*}

¹IMDEA-Water (Madrid Institute for Advanced Studies –Water), Punto Net, Edificio ZYE 2º, Parque Científico Tecnológico, 28805, Alcalá de Henares, Madrid, Spain

²National Institute for Agricultural and Food Research and Technology, INIA, 28040, Madrid, Spain

³Department of Chemical Engineering, University of Alcalá, 28871, Alcalá de Henares, Madrid, Spain

⁴Pesticide Residue Research Group, Department of Hydrogeology and Analytical Chemistry, University of Almería, 04120, Almería, Spain

RATIONALE: Polycyclic musks have become a concern due to their bioaccumulation potential and ecotoxicological effects. The HHCB transformation product (TP) (1,3,4,6,7,8-hexahydro-4,6,6,7,8,8-hexamethyl-cyclopenta[γ]-2-benzopyran; HHCB-lactone) is the most stable intermediate generated and it is frequently detected in river waters. The aim of this work was the identification of relevant TPs generated from UV irradiation and ozone treatments.

METHODS: Identification of HHCB TPs was carried out by liquid chromatography/hybrid quadrupole time-of-flight mass spectrometry (LC/ESI-QTOF-MS) and two-dimensional gas chromatography/electron impact time-of-flight mass spectrometry (GC \times GC-EI-TOF-MS). With LC/ESI-QTOF-MS, TPs were characterized by means of mass accuracy in both full-scan and MS/MS modes through information-dependent acquisition (IDA) and direct injection on-column. With stir bar sorptive extraction (SBSE)-GC \times GC-EI-TOF-MS, identification was based on the enhanced separation capacity and screening of unknowns through the acquisition of full-range mass spectra.

RESULTS: The effectiveness of these complementary techniques allowed a detailed evaluation of the main TPs. Eighteen TPs were elucidated based on mass accuracy, in both full-scan and MS/MS modes using LC/ESI-QTOF-MS with mass errors below 5 ppm and 10 ppm (mostly), respectively. Most of the TPs had not been analytically identified in previous studies. Separation of the enantiomeric species (R) and (S) of HHCB-lactone, and the identification of other relevant TPs, was performed using SBSE-GC \times GC-EI-TOF-MS.

CONCLUSIONS: LC/ESI-QTOF-MS and GC \times GC-EI-TOF-MS analysis provides the best alternative for TP identification of chemicals of concern, which have a wide range of polarities and isobaric compounds. A prediction of PBT (persistence, bioaccumulation and toxicity) using the PBT Profiler program suggested a classification of 'very persistent' and 'very toxic' for most of the TPs identified. Copyright © 2013 John Wiley & Sons, Ltd.

Synthetic musks are widely used as scent components in an extensive range of personal care products (PCPs) and other consumer products in domestic or industrial use such as cleaning or washing agents, and disinfectants. Amongst them, the market for polycyclic compounds is mainly represented by HHCB (1,3,4,6,7,8-hexahydro-4,6,6,7,8,8-hexamethylcyclopenta[γ]-2-benzopyran (GalaxolideTM))

followed by (TonalideTM). HHCB is a high production volume (HPV) chemical (in the range of 5000 to 10 000 tons) according to the European Inventory of Existing Commercial Chemical Substances.^[1] Its potential release into the environment can take place during the production phase (compounding and formulation) but it is mostly discharged with water into the sewer system after consumer use. Several monitoring studies have evidenced the presence of HHCB in untreated wastewater, sewage treatment plant (STP) effluents and sewage sludge^[2] as a consequence of suboptimal removal in STPs,^[3] although these studies are not conclusive in quantitative terms regarding HHCB biodegradation. Because of this incomplete removal, HHCB has also been detected in sediments downstream of the STPs^[2] and in surface waters in the parts

* Correspondence to: A. R. Fernández-Alba, IMDEA-Water (Madrid Institute for Advanced Studies –Water), Punto Net, Edificio ZYE 2º, Parque Científico Tecnológico, 28805 Alcalá de Henares, Madrid, Spain.
E-mail: amadeo@ual.es

per trillion (ppt) to parts per billion (ppb) range.^[3,4] Its frequent detection in aquatic environments, even more often than nitro musk compounds (NMCs), suggests a new pattern of use – that HHCB has replaced NMCs, to some extent, because of the impact of the latter on the environment.

Over recent years, polycyclic musks (PMCs) have become of emerging concern due to their bioaccumulation potential and toxicological effects although further studies are still necessary to demonstrate whether HHCB toxic effects, at the levels found in the environment, might result from bioaccumulation. Some studies carried out *in vivo* and *in vitro* suggest that HHCB may cause effects of great concern such as endocrine disruption.^[5,6] With respect to ecotoxicity, HHCB has been found to inhibit the larval development of different small aquatic crustacean species at low concentrations,^[7,8] indicating a significant toxic effect on some aquatic organisms.

To carry out environmental impact assessment, another relevant issue that needs to be addressed is the identification of transformation products (TPs). The lactone, 1,3,4,6,7,8-hexahydro-4,6,6,7,8, 8-hexamethylcyclopenta[γ]-2-benzopyran-1-one, an oxidation product of HHCB, was identified for the first time in environmental samples.^[9] Since then, screening studies have reported that the levels of HHCB and HHCB-lactone in the environment are not decreasing and frequently occur at levels similar to, or higher than, HHCB in STP effluent and surface waters downstream of STPs.^[3,10] This has been interpreted as biodegradation governed by HHCB oxidation processes towards HHCB-lactone in the STP.^[11,12] As found in preceding studies, it is also possible that HHCB-lactone can be hydroxylated to form the corresponding hydroxy acids. Several other stable intermediates detected by gas chromatography/mass spectrometry (GC/MS), or other chromatographic techniques, remain to be identified.^[13] So far, most of the studies for assessing the identification and quantification of musk fragrance degradation intermediates, including HHCB-lactone, have been based on mass spectrometry techniques such as single quadrupole mass spectrometry and, more recently, by time-of-flight mass spectrometry or tandem mass spectrometry.^[12,14,15] According to the reported data, little or no HHCB mineralization takes place, and HHCB-lactone is known to be the principal (and relatively stable) end product.^[12]

Another feature of HHCB is its chirality, which can confer different toxicological behaviour.^[16] For determining enantiomeric composition, GC/MS has been the technique of choice in HHCB analysis.^[15] Some studies have used modified cyclodextrins as chiral stationary phases coupled to high-resolution mass spectrometry enabling determination of the enantiomeric composition of HHCB ((4*S*,7*RS*)- and (4*R*,7*RS*)-HHCB) in biota reared in a pond, which receives effluents from STPs.^[9,11] However, at present, there is a lack of data regarding the detection of HHCB TP enantiomers.

The aim of this study is to provide insight into TPs generated from various oxidative and irradiation processes using liquid chromatography/hybrid quadrupole time-of-flight mass spectrometry (LC/ESI-QTOF-MS) and enantiomeric separation of TPs using comprehensive two-dimensional gas chromatography/time-of-flight mass spectrometry (GC \times GC-EL-TOF-MS). Oxidation experiments were performed with dissolved ozone and irradiation was provided by ultraviolet and visible light lamps. A comprehensive study of

fragmentation mechanisms and an elucidation of the HHCB degradation pathway are described. After elucidation of the chemical structures of TPs, a prediction of the persistence, bioaccumulation and toxicity potential was conducted using the PBT Profiler program for screening of TPs of environmental concern. The PBT Profiler, a widely used tool, can quantify and predict the fate of a chemical in the environment, and these predictions can be evaluated to prioritize chemical hazards.^[17,18]

EXPERIMENTAL

Chemicals and reagents

1,3,4,6,7,8-Hexahydro-4,6,6,7,8,8-hexamethyl-cyclopenta- γ -2-benzopyran (HHCB) (trade name: Galaxolide™ – with purity higher than 85%) was purchased from Dr. Ehrenstorfer (Augsburg, Germany). Analytical-grade ethyl acetate, methanol, acetonitrile and sodium chloride (99.5% purity) were supplied by J.T. Baker (Deventer, The Netherlands). Water used for LC/MS analysis was generated from a Direct-Q™ 5 ultrapure water system (Millipore, Bedford, MA, USA) with a specific resistance of 18.2 M Ω ·cm. Formic acid (98% purity) was purchased from Fluka (Buchs, Germany).

Sample preparation and LC/ESI-QTOF-MS analysis

The samples (40 mL) were extracted by means of solid-phase extraction (SPE). Oasis HLB (divinylbenzene/*N*-vinylpyrrolidone copolymer) cartridges (200 mg, 6 cm³; Waters, Milford, MA, USA) were used to prepare aqueous samples of the irradiation and oxidative experiments after different exposure times. The cartridges were placed in a Visiprep™ SPE vacuum manifold (Supelco, Bellefonte, USA), and washed with 3 mL of methanol plus 3 mL of deionized water, with no vacuum. Following this, the samples were extracted and the analytes, trapped in the cartridges, were eluted using 2 \times 2 mL of methanol. The extracts were evaporated until near dryness using a SBHCONC/1 sample concentrator (Stuart, Staffs, UK). The samples were then reconstituted with 1 mL of acetonitrile/water (10:90, v/v).

Data acquisition was performed with a TripleTOF 5600 hybrid quadrupole time-of-flight mass spectrometer system (AB SCIEX, Concord, ON, Canada) connected to an 1200 Series HPLC system (Agilent Technologies, Wilmington, DE, USA) with an electrospray ionization (ESI) interface, LC/ESI-QTOF-MS. The ion source parameters were: ion spray voltage floating (ISVF), 5500 V; temperature (TEM), 550 °C; curtain gas (CUR), 25 L/min and ion source gas (GS1 and GS2) at 35 psi and 40 psi, respectively. Nitrogen was used as the nebulizer gas, curtain gas and collision gas.

The MS was operated in full-scan TOF-MS and MS/MS mode through information-dependent acquisition (IDA) in a single-run analysis. In addition to the discriminative information based on mass accuracy of the molecular ion acquired in TOF-MS, MS/MS mode was used for the characterization of TPs. The declustering potential (DP) and collision energy (CE) were 70 V and 10 eV in the full-scan TOF-MS experiment. The acquisition method developed via IDA combined, simultaneously, a 250 ms TOF-MS survey scan and dependent MS/MS scans (programmed with a

maximum of 4 candidate ions to monitor per cycle). The selected IDA criteria were: (i) intensity threshold of 100 counts per second (cps) (units); (ii) mass range of 55 to 350 Da for the selection of dependent MS/MS scan candidate ions and; (iii) a mass tolerance of 50 mDa (the symmetrical window around the candidate ion was selected for MS/MS). Under these operational conditions, a collision energy spread (CES) was applied in conjunction with the CE to provide MS/MS-type scans. The result is that CE is ramped over an interval by entering a CES value (CE–CES to CE+CES). Both CE and CES were set at 35 and 20 eV, respectively (which means 35 ± 20 eV), in the first experiment and, in a second experiment, were set at 45 ± 10 eV, in order to achieve optimal fragmentation of the precursor ion and subsequent sufficient structural information in MS/MS mode. In this working mode, the accumulation time was 75 ms in dependent MS/MS scans applied for those ions of higher signal intensity found in full-scan mode. Total cycle time was fixed to 0.45 s. The advantage of applying dynamic background subtraction (DBS) criteria by IDA was to facilitate the selection of those ions that had an LC peak profile with the greatest intensity rate against background ions.

Mass calibration and resolution adjustments were performed automatically using a 10^{-5} mol/L solution of poly(propylene glycol) introduced via a syringe pump and connected to the interface. The instrument was calibrated in full-scan TOF-MS and MS/MS modes. The mass spectrometer was operated with a resolution power (RP) of approx. 20 000 FWHM (full width at half maxima) for TOF-MS scans at m/z 609.28066 ($C_{33}H_{40}N_2O_9$, reserpine). For calibration in MS/MS mode, the characteristic masses used were: $C_{11}H_{12}NO$ (174.0913), $C_{13}H_{18}NO_3$ (195.0652), $C_{13}H_{18}NO_3$ (236.1281), $C_{22}H_{25}N_2O_3$ (365.1860), $C_{23}H_{29}N_2O_4$ (397.2122) and $C_{23}H_{30}NO_8$ (448.1966). This QTOF uses an automated external calibration system for mass accuracy with an injector system (CDS, calibrant Delivery System Status) and an internal auto calibration by means of an interactive recalibration tool based on the common background ions found.

A HPLC binary solvent delivery system equipped with a reversed-phase C-18 analytical column (50 mm length 4.6 mm i.d. and 1.8 μ m particle size; Zorbax Eclipse XDB-C18, Agilent Technologies, Wilmington, DE, USA) was selected for the separation of the TPs. Mobile phases A and B were, respectively, acetonitrile and HPLC-grade water with 0.1% formic acid present in both phases. The flow rate was 600 μ L/min. A linear gradient was set from 10% to 100% of acetonitrile in 12 min, and then maintained at 100% for 5 min. The re-equilibration time was 7 min. The injection volume was 20 μ L.

The data acquisition and processing in the LC/ESI-QTOF-MS system was carried out using Analyst[®] TF 1.5 and PeakView[™] (AB SCIEX) software. For further review of data for non-target compounds, PeakView software was used. This software incorporates tools to display, filter, and process IDA data. Using the IDA Explorer application for data processing and retrospective analysis, TP characterization was performed based on accurate mass (mass error), elemental composition assignment and MS/MS spectrum interpretation. This data processing includes the matching of the experimental MS/MS spectrum with a list of theoretical fragment masses, where the threshold of mass tolerance was set lower than 15 ppm. Specialized PeakView software,

Formula Finder and Structure Elucidation tools enabled elemental composition assignment and a detailed structural interpretation of MS/MS spectrum. The MOL File application inside the PeakView software was very useful for the structural elucidation of the TPs.

Sample treatment and GC×GC-EI-TOF-MS analysis

Water sample analyses were carried out, without preliminary filtration, using stir bar sorptive extraction (SBSE) followed by comprehensive two-dimensional gas chromatography (GC×GC-EI-TOF-MS). The extraction procedure was carried out according to a previous optimized protocol.^[4] In short, the extractions were performed with PDMS commercial stir bars (20 mm length × 0.5 mm film thickness; Gerstel, Mülheim a/d Ruhr, Germany). Sodium chloride (20 g) and 10% methanol were added with the aim of improving the response of most of the analytes. The extraction was carried out at room temperature (25 °C) overnight (14 h) while stirring at 900 rpm. The coated stir bars were thermally desorbed using a commercial thermal desorption unit, TDU (Gerstel), connected to a programmed temperature vaporisation (PTV) system injector (CIS-4, Gerstel), using a heated transfer line at 300 °C. The PTV injector was installed in a GC×GC-EI-TOF-MS system, which consisted of an model 7890A gas chromatograph (Agilent Technologies, Palo Alto, CA, USA), equipped with a secondary oven to fit the secondary column, and a quad-jets modulator (two cold jets and two hot jets). The first column was a Rtx-5 (10 m × 0.18 mm i.d., 0.2 μ m) and the second column a Rxi-17 (1 m × 0.1 mm i.d., 0.10 μ m), both from Restek. The MS system was a Pegasus 4D TOF from LECO Corporation (St. Joseph, MI, USA). Electron impact (EI) mass spectra in full-scan mode were obtained at 70 eV. This analytical procedure has been previously described in detail.^[4] The chromatographic conditions were as follows: the first-dimension column oven temperature programme began at 70 °C for 3 min, then increased to 150 °C at a rate of 30 °C/min, followed by a 5 °/min ramp to 200 °C, and finally at a rate of 15 °C/min to 285 °C, and held at this temperature for 5 min – the total analysis time was 27.17 min. The second-dimension column oven temperature began at 15 °C, then 20 °C, 20 °C and finally 30 °C higher than the corresponding first-dimension column oven temperature with the same rate and hold time. The final modulation period, for our purposes, was chosen to be 4 s with 0.6 s hot pulse duration and a +25 °C modulator temperature offset against the primary oven temperature.

Oxidation of HHCB

In this study, three different experiments, based on oxidation and irradiation processes, were applied for HHCB degradation with the aim of characterizing the TPs generated in each process. These experiments were carried out on an HHCB solution at a concentration of 1 mgL⁻¹ in pure water using 2 mM phosphate buffer at pH 7.5 prepared from 0.2 M NaH₂PO₄·2H₂O and 0.2 M Na₂HPO₄ solutions to avoid pH drift.

Ozone was produced by a corona discharge (Ozomatic, 119 SWO100 fed by oxygen) and continuously bubbled throughout the run. The dissolved ozone concentration was monitored using an amperometric Rosemount 499A OZ analyzer calibrated against the standard Indigo Colorimetric

Method (SM 4500- O₃B). The gas flow, under normal conditions (N, 1 atm and 273.15 K), was 0.19 N m³ h⁻¹ containing 22 g N m⁻³ ozone. The ozonation runs were carried out in a 1.3 L glass-jacketed reactor operating at 25 °C, the temperature being kept constant by means of a Huber Polystat cc2 unit.

Irradiation experiments were performed using a 15 W Heraeus Noblelight TNN 15/32 low-pressure mercury vapour lamp emitting at 254 nm and a Heraeus TQ Xe 150 Xe-arc lamp with emission in the visible region. For visible light irradiation, an additional Pyrex tube acted as a filter absorbing wavelengths <290 nm. The lamp sleeve was equipped with a quartz cooling tube, in which the lamps were fitted, and was refrigerated by means of a thermostatic bath. The temperature was kept at 25 °C. The pH was kept constant a 7.5 within ±0.1 units. For Xe lamp irradiation runs, a photocatalyst was used that consisted of ceria-doped TiO₂ (0.5% wt. of cerium) prepared using the sol-gel method as described elsewhere.^[19] The bulk concentration of catalyst was 200 mg L⁻¹ kept suspended with a magnetic stirrer operating at 900 min⁻¹. The reason for using a photocatalyst is that the use of visible light irradiation alone on HHCB did not lead to any significant degradation. Details on the photocatalyst and on the actinometric characterization of both irradiation processes as well as the experimental set-up can be found in a previous work.^[19]

RESULTS AND DISCUSSION

Identification of TPs by LC/ESI-QTOF-MS analysis

Data on HHCB occurrence in all compartments of the aquatic environment, as well as in biota, are consistent with its lipophilic and persistent nature.^[20] The degradation half-life is around 100 days in river samples and 150–200 days under laboratory-based conditions.^[20] Biodegradation tests have demonstrated that HHCB leads to the formation of 1,3,4,6,7,8-hexahydro-4,6,6,7,8,8-hexamethylcyclopenta[*γ*]-2-benzopyran-1-one (HHCB-lactone) as a relatively stable end product of HHCB metabolism.^[20,21] Photooxidative studies have also suggested a similar pattern towards the formation of other polar metabolites, by HHCB hydroxylation, to form the corresponding hydroxy acid. Other stable intermediates have been suggested, but they have not been identified.^[13,22]

In this work, we have explored TP characterization generated under oxidative and irradiation conditions.

The rate of HHCB depletion was high using ozone, with over 98% removal after 2 min. The rate constant for the HHCB reaction with molecular ozone is relatively low, 8 M⁻¹ s⁻¹, but the absence of competing substances makes removal particularly efficient in pure water.^[19] Irradiation processes were less efficient in removing HHCB with depletion over 80% after 2 min under UV irradiation. We showed in a previous work^[19] that HHCB depletion in a wastewater matrix was relatively rapid in ozone-based treatments, while UV photolysis gave poor results (<60% removal after 15 min). The difference, with respect to pure water runs, can be explained by the presence of UV-absorbing compounds in wastewater. Visible light irradiation of HHCB in the presence of the Ce-TiO₂ photocatalyst also resulted in high removal efficiency. Using the wastewater matrix, we also

noted that Xe/Ce-TiO₂ was able to efficiently remove HHCB even though its ability to produce hydroxyl radicals was relatively low.^[19] In all cases, samples were withdrawn after 8 min of oxidation or irradiation with the aim of identifying the TP produced in each process.

The TPs identified by LC/ESI-QTOF-MS analysis of the water samples obtained from the lab-scale studies performed with O₃, UV and Xe are listed in Table 1. Structural elucidation of TPs was achieved by accurate mass measurement in both full-scan and MS/MS modes by means of IDA in a single-run analysis.

TPs with *m/z* 273

HHCB degradation towards HHCB-lactone was observed as a dominant pathway to oxidation in the three treatments. As an example, Fig. 1(A) shows an intense peak at retention time (Rt) 12.09 min and the full-scan mass spectrum with the ion at *m/z* 273.1852, corresponding to the O₃ treatment after 5 min.

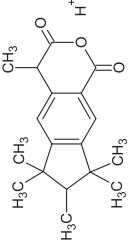
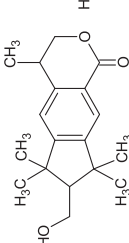
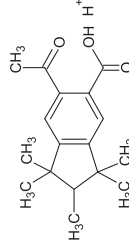
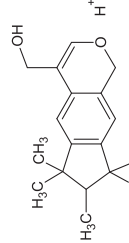
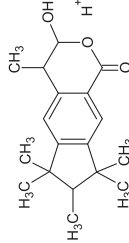
To assign elemental composition and to perform structure-based fragment interpretation, we made use of formula finder and structure elucidation. Formula finder provided only one proposal with an elemental composition of C₁₈H₂₅O₂⁺, based on a measured mass at *m/z* 273.1852 with an error of 1.1 ppm and a ring plus double bond (RBD) factor of 6.5 – this, therefore, was preliminarily assigned to HHCB-lactone.

IDA explorer provided a list of all fragment ions as well as the mass errors. Figure 1(B) shows the TOF-MS/MS spectrum from the peak at Rt 12.09 min and the proposed formula composition fragment ions. By applying the structure elucidation application, a proposed structure (mol file) could be linked to the spectrum obtained and provides insight into the fragmentation mechanisms. Following this, all fragment ions which match with the proposed molecule, based on elemental composition and mass error, mostly those with a relative intensity higher than 30%, are highlighted. From the precursor ion at *m/z* 273.1, the fragment ions observed by decreasing relative intensity were: 225.1297(100), 197.1341(78), 255.1768(46), 212.1576(36), 240.1532(33), 129.0701(32) and 157.1015(32).

HHCB-lactone is degraded through the formation of hydroxyl radicals. Hydroxyl radicals are generated from the decomposition of ozone or from the action of visible light on the surface of the Ce-TiO₂ photocatalyst. Peroxide moieties are subsequently formed by the addition of molecular oxygen followed by protonation, removal of a water molecule and rupture of the ring. This leads to the formation of an acylium fragment (*m/z* 255.1768, C₁₈H₂₃O⁺, 9.5 ppm). The sequential loss of two methyl groups leads to *m/z* 225.1297 (C₁₆H₁₇O⁺, 10.2 ppm), the fragmentation of which results in the loss of a carbonyl group and the formation of *m/z* 197.1341 (C₁₅H₁₇⁺, 8.2 ppm). From the acylium fragment at *m/z* 255.1768, a second fragmentation mechanism results in the consecutive loss of a methyl radical yielding the radical ion *m/z* 240.1532 (C₁₇H₂₀O⁺, 9.8 ppm) and the posterior loss of a carbonyl group, *m/z* 212.1576 (C₁₆H₂₀⁺, 7.8 ppm).

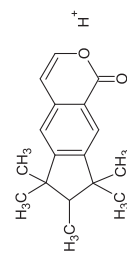
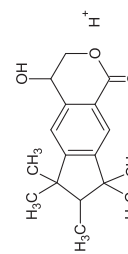
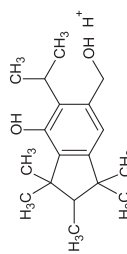
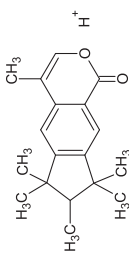
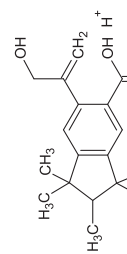
In Fig. 1(A), two peaks at Rt 11.91 and 12.23 min are detected in all treatments close to the peak at Rt 12.09 min (HHCB-lactone). The peak at Rt 11.91 min, with *m/z* 273.1853, was assigned to C₁₈H₂₅O₂⁺ with a mass error of 1.4 ppm and 6.5 RDB. This TP was identified as a structural isomer of HHCB-lactone because its spectrum only differs from the spectrum at Rt 12.09 min in the relative intensity of common

Table 1. Structural elucidation of 18 transformation products generated during treatments with ozone, UV and Xe by LC/ESI-QTOF-MS analysis. Identification criteria based on accurate mass measurements of molecular ions and fragment ions and fragment ions, elemental composition assignment and ring and double bonds (RDB)

TOF-MS		TOF-MS/MS										
Rt (min)	TP	Measured mass (Da)	Elemental composition ([M+H] ⁺)	RDB ^d	Theoretical mass (Da)	Error (ppm)	TIC – Peak intensity ^e	Major fragment ions (Relative intensity, %)	Elemental composition of fragment ions	Error (ppm)	log K _{ow} ^f	Proposed structure
8.16 ^a	1	287.1642	C ₁₈ H ₂₃ O ₃ ⁺	7.5	287.1642	0.1	5.1 × 10 ³	195.1168(100) 129.0714(38) 168.0934(25) 179.0879(25) 231.1033(13)	(C ₁₅ H ₁₅) (C ₁₀ H ₈) (C ₁₃ H ₁₂) (C ₁₄ H ₁₁) (C ₁₄ H ₁₅ O ₃ ⁺)	2.1 12 0.5 13 7.3	6.37	
8.25 ^a	2	289.1808	C ₁₈ H ₂₅ O ₃ ⁺	6.5	289.1798	3.4	8.5 × 10 ³	225.1271(100) 271.1674(40) 197.1336(33) 142.0781(11) 185.0940(11) 256.1465(11)	(C ₁₆ H ₁₇ O ⁺) (C ₁₈ H ₂₃ O ₂) (C ₁₅ H ₁₇) (C ₁₁ H ₁₀) (C ₁₃ H ₁₃ O ⁺) (C ₁₇ H ₂₀ O ₂ ⁺)	1.5 7 5.5 2.6 11.5 2.9	3.79	
8.30 ^a	3	275.1649	C ₁₇ H ₂₃ O ₃ ⁺	7.5	275.1642	2.5	1.3 × 10 ⁴	217.1253(100) 141.0701(67) 187.1124(54) 159.0790(53) 157.1006(52)	(C ₁₄ H ₁₇ O ₂) (C ₁₁ H ₉) (C ₁₃ H ₁₅ O ⁺) (C ₁₁ H ₁₁ O ⁺) (C ₁₂ H ₁₃)	13.0 6.3 0.9 13.0 3.4	4.84	
10.00 ^b	4	273.1859	C ₁₈ H ₂₅ O ₂ ⁺	6.5	273.1849	3.6	9.8 × 10 ⁴	255.1757(100) 143.0860(93) 128.0637(66) 185.0971(52) 157.1027(45) 171.0810(43)	(C ₁₈ H ₂₃ O ⁺) (C ₁₁ H ₁₁) (C ₁₀ H ₈) (C ₁₃ H ₁₃ O ⁺) (C ₁₂ H ₁₃) (C ₁₂ H ₁₁ O ⁺)	4.0 3.2 13 5.6 9.9 3.1	4.71	
10.22 ^{ab}	5	289.1796	C ₁₈ H ₂₅ O ₃ ⁺	6.5	289.1798	-0.8	7 × 10 ³	243.1730(100) 271.1714(68) 213.1303(23) 185.1308(18) 173.0959(14)	(C ₁₇ H ₂₃ O ⁺) (C ₁₈ H ₂₃ O ₂) (C ₁₅ H ₁₇ O ⁺) (C ₁₄ H ₁₇) (C ₁₂ H ₁₃ O ⁺)	5.4 8 13.4 8.9 0.8	4.91	

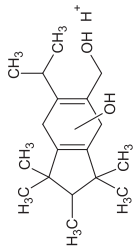
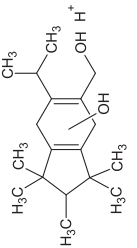
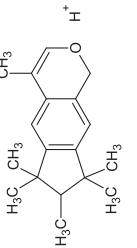
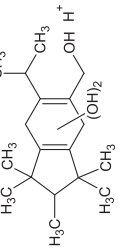
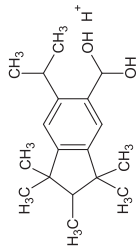
(Continues)

Table 1. (Continued)

		TOF-MS					TOF-MS/MS					
Rt (min)	TP	Measured mass (Da)	Elemental composition (M+H) ⁺	RDB ^d	Theoretical mass (Da)	Error (ppm)	TIC - Peak intensity ^e	Major fragment ions (Relative intensity, %)	Elemental composition of fragment ions	Error (ppm)	log K _{ow} ^f	Proposed structure
10.37 ^{abc}	6	257.1551	C ₁₇ H ₂₁ O ₂ ⁺	7.5	257.1536	4.6	1.7 × 10 ⁴	227.1066 (100) 212.0822 (26) 197.0615 (23) 141.0691 (16) 199.1118 (11)	(C ₁₅ H ₁₅ O ₂ ⁺) (C ₁₄ H ₁₂ O ₂ ⁺) (C ₁₃ H ₉ O ₂ ⁺) (C ₉ H ₁₁) (C ₁₄ H ₁₅ O ⁺)	0.3 4.7 9.0 5.5 0.2	5.38	
10.46 ^{abc}	7	275.1633	C ₁₇ H ₂₃ O ₃ ⁺	6.5	275.1642	-3.2	4.9 × 10 ³	257.1542 (100) 227.1085 (67) 242.1303 (15) 199.1089 (11) 212.0834 (11)	(C ₁₇ H ₂₁ O ₂ ⁺) (C ₁₅ H ₁₅ O ₂ ⁺) (C ₁₆ H ₁₈ O ₂ ⁺) (C ₁₄ H ₁₅ O ⁺) (C ₁₄ H ₁₂ O ₂ ⁺)	2.2 8.0 0.7 14.5 1.2	3.30	
10.40 ^{abc}	8	277.2165	C ₁₈ H ₂₉ O ₂ ⁺	4.5	277.2162	-1.1	1.3 × 10 ⁴	79.0534 (100) 93.0692 (77) 77.0387 (68) 91.0545 (59) 107.0847 (50) 135.1161 (32) 241.1971 (14)	(C ₆ H ₇ ⁺) (C ₇ H ₉) (C ₆ H ₅) (C ₇ H ₇ ⁺) (C ₈ H ₁₁) (C ₁₀ H ₁₅) (C ₁₈ H ₂₅)	11.0 7.8 1.6 3.3 7.5 5.2 8.5	4.83	
10.70 ^{bc}	9	271.1700	C ₁₈ H ₂₃ O ₂ ⁺	7.5	271.1693	2.7	4.5 × 10 ⁴	241.1232 (100) 213.0909 (30) 211.0774 (28) 227.1077 (21) 187.0742 (19) 256.1477 (18)	(C ₁₆ H ₁₇ O ₂ ⁺) (C ₁₄ H ₁₃ O ₂) (C ₁₄ H ₁₁ O ₂ ⁺) (C ₁₅ H ₁₅ O ₂ ⁺) (C ₁₂ H ₁₁ O ₂) (C ₁₇ H ₂₀ O ₂ ⁺)	3.6 0.6 9.8 4.4 6.0 7.6	5.93	
10.75 ^{bc}	10	289.1790	C ₁₈ H ₂₅ O ₃ ⁺	6.5	289.1798	-2.8	9.8 × 10 ³	271.1696 (100) 241.1214 (30) 213.0907 (17) 256.1460 (7) 201.0916 (6)	(C ₁₈ H ₂₃ O ₂ ⁺) (C ₁₆ H ₁₇ O ₂ ⁺) (C ₁₄ H ₁₃ O ₂ ⁺) (C ₁₇ H ₂₀ O ₂) (C ₁₃ H ₁₃ O ₂ ⁺)	1.3 3.9 1.5 0.8 3.1	5.14	

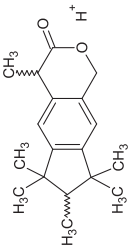
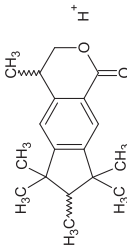
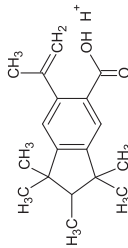
(Continues)

Table 1. (Continued)

		TOF-MS/MS										
		TOF-MS										
Rt (min)	TP	Measured mass (Da)	Elemental composition ([M+H] ⁺)	RDB ^d	Theoretical mass (Da)	Error (ppm)	TIC – Peak intensity ^e	Major fragment ions (Relative intensity, %)	Elemental composition of fragment ions	Error (ppm)	log K _{ow} ^f	Proposed structure
11.08 ^a	11	279.2321	C ₁₈ H ₃₁ O ₂ ⁺	3.5	279.2319	0.9	3.6 × 10 ⁴	67.0552(100) 81.0705(68) 95.0852(65) 79.0543(23) 109.1008(18) 261.2187(5.5) 243.2128(4.4)	(C ₅ H ₇ ⁺) (C ₆ H ₉ ⁺) (C ₇ H ₁₁ ⁺) (C ₆ H ₇ ⁺) (C ₈ H ₁₃ ⁺) (C ₁₈ H ₂₉ O ⁺) (C ₁₈ H ₂₇)	14.4 7.5 3.4 1.2 3.7 10 8.4	5.10	
11.27 ^a	12	279.2317	C ₁₈ H ₃₁ O ₂ ⁺	3.5	279.2319	-0.6	1.6 × 10 ⁴	67.0546(100) 95.0849(94) 81.0702(72) 79.0546(39) 93.0707(22) 261.2193(3)	(C ₅ H ₇ ⁺) (C ₇ H ₁₁ ⁺) (C ₆ H ₉ ⁺) (C ₆ H ₇ ⁺) (C ₇ H ₉ ⁺) (C ₁₈ H ₂₉ O ⁺)	5.0 6.6 4.2 5.0 9.4 7.8	5.10	
11.43 ^{abc}	13	257.1912	C ₁₈ H ₂₅ O ⁺	6.5	257.1900	4.7	2.8 × 10 ⁵	227.1455(100) 209.1315(47) 141.0709(33) 169.1024(24) 187.1126(24) 194.1079(22)	(C ₁₆ H ₁₉ O ⁺) (C ₁₆ H ₁₇) (C ₁₇ H ₉ ⁺) (C ₁₃ H ₁₃ ⁺) (C ₁₃ H ₁₅ O ⁺) (C ₁₅ H ₁₄ ⁺)	10.9 10.2 7.5 7.1 4.6 5.7	6.17	
11.55 ^{abc}	14	295.2255	C ₁₈ H ₃₁ O ₃ ⁺	3.5	295.2268	-4.6	1.2 × 10 ⁴	277.2127(100) 79.0535(44) 91.0544(44) 93.0694(44) 151.1131(44) 71.0855(33) 99.0801(33) 259.2027(11) 241.1968(11) 93.0690(78) 79.0539(56) 77.0390(44) 121.1008(44) 91.0540(34) 105.0693(34) 241.1926(8)	(C ₁₈ H ₂₉ O ₂ ⁺) (C ₆ H ₇ ⁺) (C ₇ H ₉ ⁺) (C ₇ H ₉) (C ₁₀ H ₁₅ O ⁺) (C ₅ H ₁₁ ⁺) (C ₆ H ₁₁ O ⁺) (C ₁₈ H ₂₇ O ⁺) (C ₁₈ H ₂₅) (C ₇ H ₉) (C ₆ H ₇ ⁺) (C ₆ H ₅ ⁺) (C ₉ H ₁₃) (C ₇ H ₇ ⁺) (C ₈ H ₉ ⁺) (C ₁₈ H ₂₅)	1.9 9.7 1.8 5.2 8.7 0.0 3.9 11.4 7.3 9.2 4.5 4.9 2.8 3.0 5.5 10.3	5.20	
11.52 ^a	15	277.2150	C ₁₈ H ₂₉ O ₂ ⁺	4.9	277.2162	-4.4	4.9 × 10 ³				5.93	

(Continues)

Table 1. (Continued)

TOF-MS		TOF-MS/MS										
Rt (min)	TP	Measured mass (Da)	Elemental composition (M+H) ⁺	RDB ^d	Theoretical mass (Da)	Error (ppm)	TIC - Peak intensity ^e	Major fragment ions (Relative intensity, %)	Elemental composition of fragment ions	Error (ppm)	log K _{ow} ^f	Proposed structure
11.91 ^{abc}	16	273.1853	C ₁₈ H ₂₅ O ₂ ⁺	6.5	273.1849	1.4	6.9 × 10 ⁴	225.1278(100) 255.1763(87) 129.0692(83) 157.1020(60) 142.0767(59) 197.1334(47)	(C ₁₆ H ₁₇ O ⁺) (C ₁₈ H ₂₃ O ⁺) (C ₁₀ H ₅) (C ₁₂ H ₁₃) (C ₁₁ H ₁₀) (C ₁₅ H ₁₇)	1.9 7.5 5.3 5.1 7.2 4.8	5.01	
12.09 ^{abc}	17	273.1852	C ₁₈ H ₂₅ O ₂ ⁺	6.5	273.1849	1.1	7.3 × 10 ⁵	225.1297(100) 197.1341(78) 255.1768(46) 212.1576(36) 240.1532(33) 129.0701(33)	(C ₁₆ H ₁₇ O ⁺) (C ₁₅ H ₁₇) (C ₁₈ H ₂₃ O ⁺) (C ₁₆ H ₂₀) (C ₁₇ H ₂₀ O ⁺) (C ₁₀ H ₅)	10.2 8.2 9.5 7.8 9.8 1.6	5.25	
12.23 ^{abc}	18	273.1854	C ₁₈ H ₂₅ O ₂ ⁺	6.5	273.1849	1.8	7.8 × 10 ³	211.1142(100) 183.1171(74) 226.1362(68) 255.1724(47) 129.0694(33) 155.0854(27) 128.0620(22) 168.0943(22)	(C ₁₅ H ₁₅ O ⁺) (C ₁₄ H ₁₅) (C ₁₆ H ₁₈ O ⁺) (C ₁₈ H ₂₃ O ⁺) (C ₁₀ H ₅) (C ₁₂ H ₁₁) (C ₁₀ H ₈) (C ₁₃ H ₁₂)	11.4 1.7 4.3 7.5 4.0 1.1 0.4 5.6	6.61	

^aTPs by ozone treatment.

^bTPs by UV treatment.

^cTPs by Xe/Cat treatment.

^dRDB, rings and double bonds.

All RDB presented in the table correspond to the even electron ions.

^eTIC- peak intensity shows "relevant TPs" in terms of abundance.

^flog Kow - calculated by the PBT Profiler program.

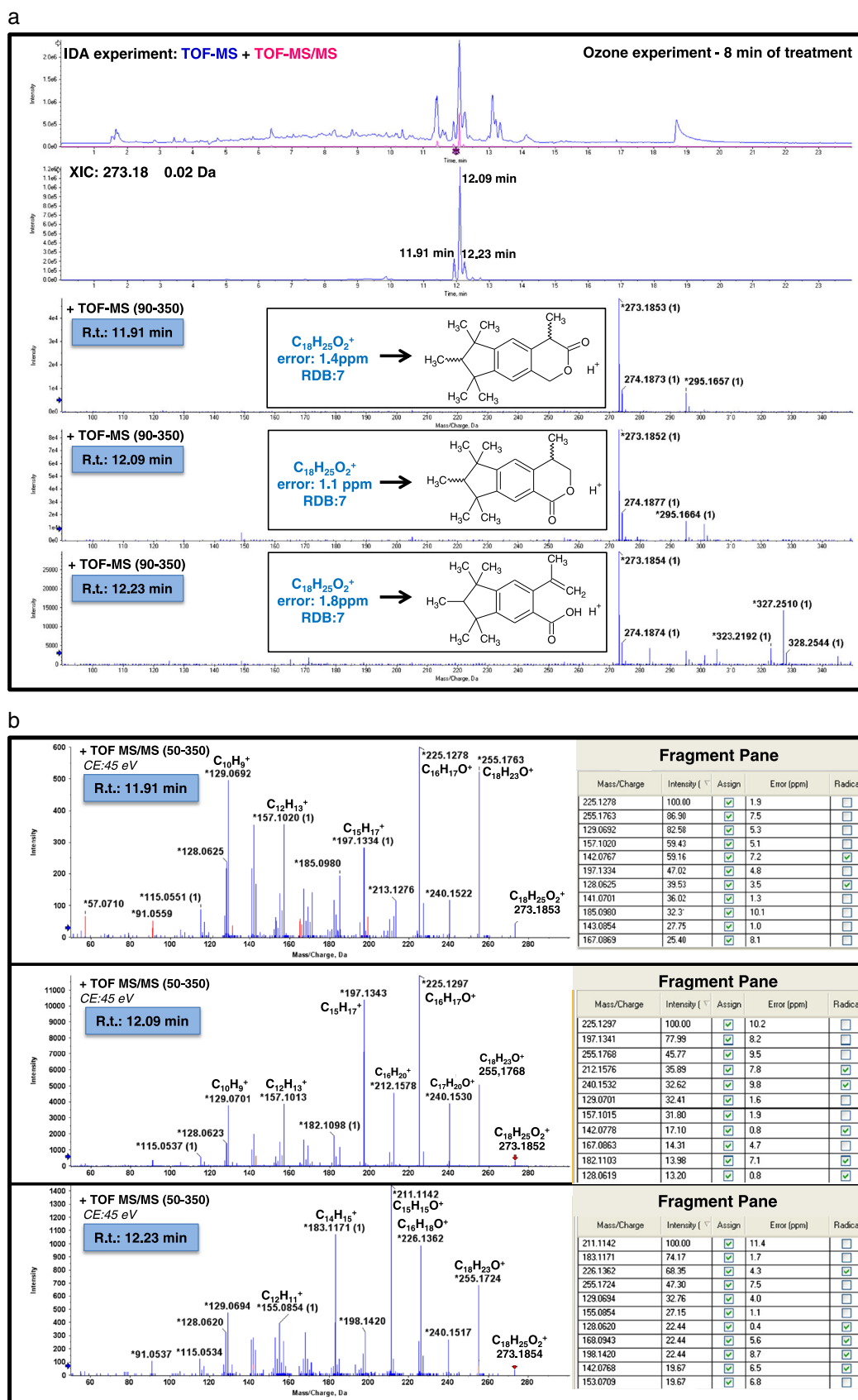


Figure 1. Identification of three transformation products of HHCb with the same mass 273.18 by LC/QTOF-MS. (A) Chromatographic separation at different Rt, total ion chromatogram (TIC), extracted ion chromatogram (XIC) and full-scan spectra. (B) Overlay of experimental MS/MS spectra and theoretical fragmentation providing a list of structural fragments with corresponding mass error.

fragment ions. Figure 1(B) shows the LC/ESI-QTOF-MS/MS spectrum at *Rt* 11.91 min. The detection of this isomer is justified because of the HHCB-lactone structure, which has two chiral centres and four enantiomers. It is also due to the chromatographic conditions as no special column was used to separate chiral compounds – so they could not be detected by LC/MS analysis. For this reason, a structural isomer (TP-16) has been proposed instead of enantiomers. Table 1 includes the 18 polar TPs identified by LC/ESI-QTOF-MS analysis, which were generated under the three irradiation and oxidative processes. The chromatographic separation of enantiomers by GC×GC-EI-TOF-MS is described in the next section.

At *Rt* 12.23 min, *m/z* 273.1854 ($C_{18}H_{25}O_2^+$, 1.8 ppm and RDB of 6.5) initially could also be assigned to the HHCB-lactone isomer, but it was discarded due to significant differences in the LC/ESI-QTOF-MS/MS spectrum, in which several new fragment ions were observed. Table 1 presents the list of all assigned fragment ions and mass errors corresponding to TP-18. The LC/ESI-QTOF-MS/MS spectra of TP-18 exhibits *m/z* 211.1142 as the most intense product ion ($C_{15}H_{15}O^+$, 11.4 ppm). This ion resulted from the successive loss of water to form (M-18) species at *m/z* 255.1724, an ethyl radical and a methyl radical. The formation of *m/z* 183.1171 ($C_{14}H_{15}^+$, 1.7 ppm) takes place as a result of the loss of a carbonyl group (C=O). Consequently, the MS/MS spectra of TP-18 compared to the MS/MS spectra of TP-17 (HHCB-lactone) demonstrated that these ions are not identical in structure, as TP-18 does not share the closed-ring structure of HHCB (Figs. 1(A) and 1(B)).

In addition to the above-mentioned intermediates elucidated for mass 273, the LC/ESI-QTOF-MS analysis corresponding to the UV-irradiated sample shows another intense peak at *Rt* 10.00 min (TP-4) with the same mass and elemental composition ($C_{18}H_{25}O_2^+$, 3.6 ppm and RDB of 6.5). This, solely detected in the UV treatment, is another species strongly linked to the introduction of a hydroxyl group instead of the formation of higher oxidation states such as TP-16, TP-17 and TP-18, observed during ozone oxidation.

TPs with *m/z* 289

In the LC/ESI-QTOF-MS analysis, three different peaks were detected at *m/z* 289 – *Rt* 8.25 (TP-2), 10.22 (TP-5), 10.75 (TP-10) min (Table 1). TP-2 was observed in the ozone treatment, TP-5 in both UV and ozone treatments, and TP-10 in the UV experiment. For TP-2 and TP-5, an identical elemental composition of $C_{18}H_{25}O_3^+$ matched with an error of 3.4 ppm (TP-2) and –0.8 ppm (TP-5); and with 6.5 RDB – using IDA explorer, several differences arose between the MS/MS spectra.

TP-2 corresponds to the hydroxylation of HHCB-lactone in the methyl groups of the cyclopentane ring. TP-2 is fragmented with the loss of H_2O , leading to the formation of a fragment ion at *m/z* 271.1674 ($C_{18}H_{25}O_2^+$, 7 ppm) and the posterior loss of a methyl radical, leading to a minor fragment ion at *m/z* 256.1465 ($C_{17}H_{20}O_2^+$, 2.9 ppm). The base peak at *m/z* 225.1271 ($C_{16}H_{17}O^+$) is due to the loss of CH_2OH . The subsequent loss of CO resulted in the signal observed at *m/z* 197.1336 ($C_{15}H_{17}^+$, 5.5 ppm).

In TP-5, the hydroxylation takes place in the cyclohexane ring. This degradation generates two abundant ions in the MS/MS spectra at *m/z* 271.1714 (attributed to the loss of H_2O) and 243.1730 (loss of CO and formation of a ring) confirming the proposed structure.

This fragmentation pattern was also observed in TP-10, only detected in the UV treatment. The precursor ion $[M+H]^+$ at *m/z* 289.1786 dissociated into *m/z* 271.1696, 241.1214 and 213.0907. The ion at *m/z* 271 ($C_{18}H_{23}O_2^+$), which is the base peak of the MS/MS spectrum, was generated by the loss of a water molecule. The intensity of this peak can be attributed to resonance stabilization. Consecutive losses of methyl groups in the cyclopentane ring led to the signal at *m/z* 241.1214. The subsequent loss of C_2H_4 resulted in *m/z* 213.0907.

In the above-mentioned TPs, the predominant fragmentations were marked by the loss of methyl groups, the formation of an acylium fragment and the loss of a carbonyl group. This pattern was observed in the rest of the MS/MS spectra of the TPs, for which the most abundant fragmentation mechanisms were the loss of aliphatic groups (CH_3 , C_2H_4 , C_2H_2 , C_2H_6) – as observed in TP-9, and some of them in TPs 6, 7, 11, 12. TP-7 showed the characteristic water loss. Other losses were also recognized such as $C_3H_3O_2$ in TP-7; $C_4H_2O_2$ in TP-6; and C_3H_6O , $C_2H_4O_2$ or $C_6H_{14}O_3$ in TP-3. Table 1 presents the structures of these TPs and a list of all assigned product ions used for structural elucidation, most of them with a mass error below 10 ppm. This table provides the intensity of the peaks in the TIC (total ion chromatogram) corresponding to each TP, which is related to their 'relevance' in terms of concentration. In decreasing order, the first five TPs were TP-17 (HHCB-lactone), TP-13, TP-4, TP-16 and TP-4.

Separation of enantiomers and TP identification by GC×GC-EI-TOF-MS analysis

Up to now, the most intensively studied chiral compounds have been persistent organic pollutants (POPs) – preferably using cyclodextrin as chiral stationary phase (CSP), high-resolution gas chromatography (HRGC) or modified cyclodextrin.^[23] For the separation of the musk compounds, columns with films containing 5% phenyl in dimethylsilylsiloxane such as DB-5 are frequently used, but, if separation of HHCB enantiomers is desired, the use of a 1:1 stationary phase mixture of OV 1701/heptakis(6-*O*-*tert*-butyldimethylsilyl)-2,3-di-*O*-methyl)- β -cyclodextrin provides optimal performance. Enantioselective analysis of HHCB and quantification was first established by Franke *et al.*^[9] for fish samples enabling the determination of HHCB ((4*S*,7*RS*)- and (4*R*,7*RS*)-HHCB). Previous studies^[11,24–26] reported on the enantiomer ratios of HHCB in environmental samples. Despite a variety of chiral GC columns being available, enantioselective resolution can be difficult when a single CSP column is used; this is due to an overlapping of the enantiomers of different isomers or because of other commonly encountered co-elution problems which are dependent on the matrix. To overcome the co-elution problem, comprehensive two-dimensional gas chromatography (GC×GC) has attracted attention because of its great separation efficiency. GC×GC-EI-TOF-MS appears ideal in screening a large number of compounds, target and unknowns, simultaneously, of complex environmental samples since TOFMS provides full-range mass spectra for all the sample components. In this way, a 3D-structured contour plot was obtained, where four stereoisomers of HHCB-lactone were resolved, and two of their diastereoisomers [*trans*-(4*S*,7*S*)-HHCB and *cis*-(4*S*,7*R*)-(-)-HHCB] exhibited significant differences in intensity (Fig. 2(A)). Studies regarding the enantioselective separation of

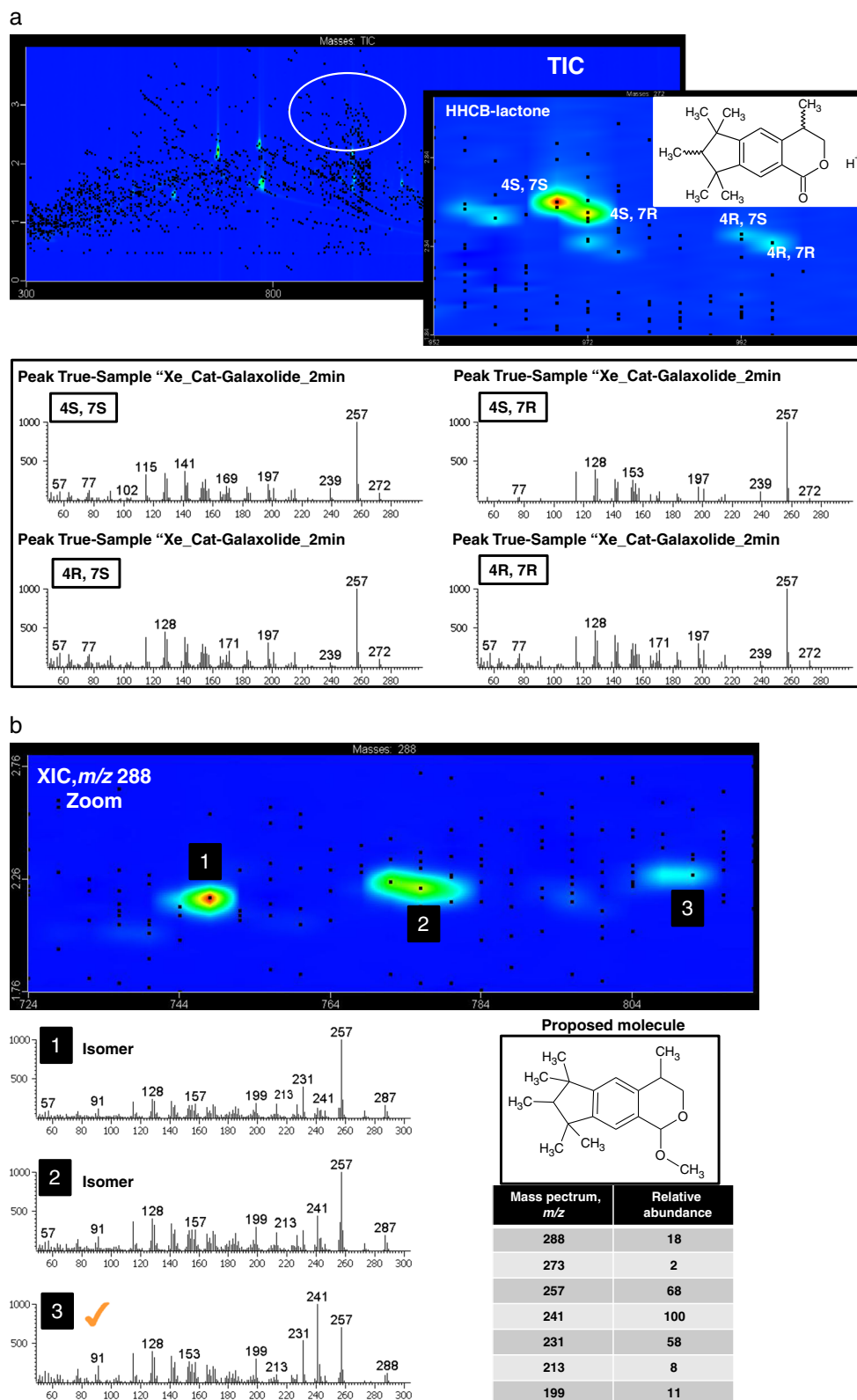


Figure 2. GC \times GC-TOFMS contour plot of a sample with ozone treatment. (A) Enantiomeric separation of *trans*-HHCB-lactone (4*S*,7*S* and 4*R*,7*R*) and *cis*-HHCB-lactone (4*S*,7*R* and 4*R*,7*S*). (B) GC \times GC-TOFMS contour plot zoom of mass 288 and full-scan spectra of three isomers detected.

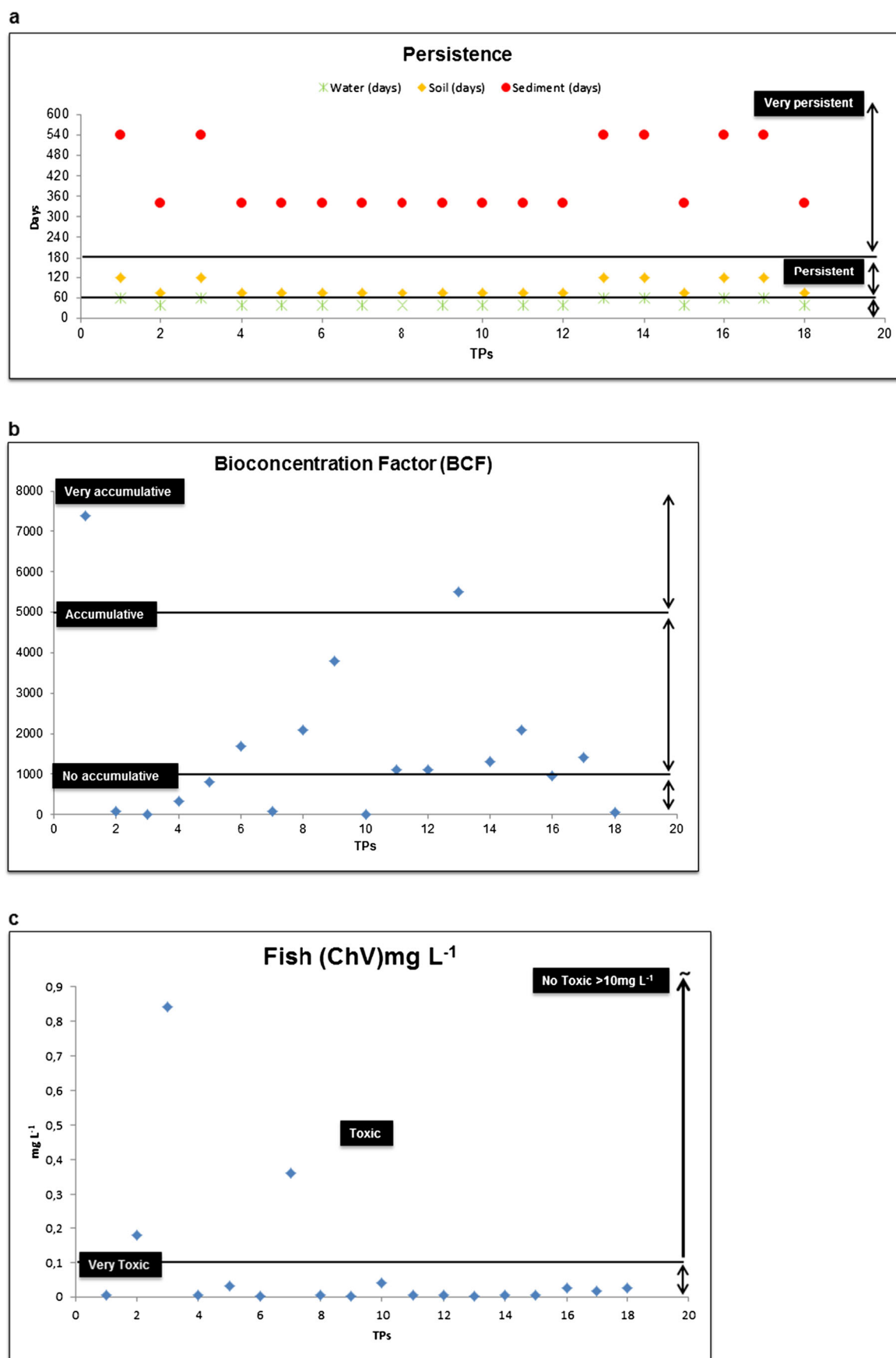


Figure 3. Estimation of (A) persistence, (B) bioaccumulation and (C) toxicity of the TPs identified by using the PBT Profiler program.

transformation products, which are very scarce,^[24] reported the enantioselective separation of HHCB-lactone using modified cyclodextrins in capillary gas chromatography (cGC) providing remarkable selectivity. However, in trace compound analysis, it is important to choose a sensitive and highly selective detection method, especially in screening analyses identifying non-target or unknown contaminants. GC×GC-EI-TOF-MS fulfils both criteria providing insights into reliable identification based on structural information. Due to the enhanced separation capacity, problems associated with co-eluting matrix compounds were largely eliminated and what would otherwise overlap in 1D-GC is separated.

TP-19 was identified by GC×GC-EI-TOF-MS analysis, based on the enhanced separation capacity; which, using conventional chromatography, might easily have led to misidentification, simplifying enantioselective data or the presence of isomers, generating greater certainty for identification purposes. The suitability of GC×GC-EI-TOF-MS for non-target analyses in terms of pollutant mapping was demonstrated facilitating the detection of three isomers at *m/z* 288 at different R_ts (Fig. 2(B)). The GC×GC-EI-TOF-MS spectrum of the three isomers fits the structure of a TP previously described by Martin *et al.*,^[27] generating microbial degradation, which supports a possible common oxidation with ozone treatment.

PBT characterization of TPs

PBTs are compounds that are toxic, persist in the environment and bioaccumulate in food chains. For the PBT Profiler program, the US Environmental Protection Agency (EPA) has developed thresholds. The tool includes methods for estimating environmental persistence (P), bioconcentration potential (B), and aquatic toxicity (T) using models that are either fragment or Kow based QSARs, or expert systems, or some combination of the three. Estimated Kow values are presented in Table 1. The PBT Profiler predictions obtained for the identified TPs are shown in Fig. 3. All TPs were very persistent in sediments and persistent in soil (see Fig. 3(A); the threshold for 'persistence' being 60–180 days, 'very persistent' being >180 days). In water, the TPs were not persistent, except TPs 1, 3, 13, 14, 16 and 17, which presented persistence (<60 days), among them HHCB-lactone. Concerning bioaccumulation, most of the TPs were accumulative except TPs 2, 3, 4, 7, 10 and 18 (see Fig. 3(B); the threshold for 'accumulative' being a BCF within the 1000–5000 range; 'very accumulative', a BCF >5000). TP-1 and TP-13 presented very high BCF values, which show they are very accumulative. The ChV factor was less than 0.1 mg L⁻¹ for most of the TPs, and, therefore, 'very toxic'. Only TP-2 and TP-7 showed values between 0.1–10 mg L⁻¹, which denote a classification as 'toxic' compounds. TP-3 is the only TP for which 'no toxicity' was predicted (Fig. 3 (C)). When chemical-specific data is lacking, such as in the case of TPs, the PBT Profiler can help to identify an issue of potential concern, but it should be considered only as supplementary information to experimental data. This software is useful in establishing priorities for chemical safety evaluation, and as a screening level predictive tool for the identified TPs providing a preliminary assessment on the potential for persistence, bioaccumulation and toxicity. For more accurate risk assessment of TPs, additional data should be gathered and/or additional experimental analyses conducted.

CONCLUSIONS

The identification of 'relevant TPs or metabolites' in terms of occurrence or concern are being considered in monitoring programmes, not only in scientific works, but also by river management organizations and water suppliers. This work demonstrated that a combined strategy, using LC/ESI-QTOF-MS and GC×GC-EI-TOF-MS analysis, provides an interesting alternative to fill the knowledge gaps related to the identification of TPs as chemicals of concern; since they can often display, not just a higher water solubility, but also greater persistence and accumulation. This might explain a detection frequency even higher than their parent compounds, such as HHCB-lactone. In this study, the structures of 18 polar TPs have been elucidated based on LC/ESI-QTOF-MS analysis, most of which have not yet been reported previously. The separation of enantiomeric species (*R*) and (*S*) of the TP HHCB-lactone and the identification of other relevant TPs was performed by SBSE-GC×GC-EI-TOF-MS analysis. A prediction of the potential PBT (persistence, bioaccumulation and toxicity) was conducted using the PBT Profiler program suggesting a classification of 'very persistent' and 'very toxic' for most of the TPs identified.

Acknowledgements

The authors acknowledge the Spanish Ministry of Science and Innovation (Project CTM2011-27657) and Programa Consolider Ingenio 2010 (CE-CSD2006-00044) for its economic support. Sonia Herrera acknowledges the 'Subprograma de Personal Técnico de Apoyo' from The Spanish Ministry of Science and Technology. Javier Santiago-Morales would like to thank the Spanish Ministry of Education for the award of an FPU grant.

REFERENCES

- [1] EINEC – European Inventory of Existing Commercial Chemical Substances. Joint Research Centre. Available: <http://esis.jrc.ec.europa.eu/index.php?PGM=hpv>.
- [2] Rapporteur TemaNord 2004:503. Nordic Council of Ministers, ISBN 92-893-0981-4. Available: <http://nordicscreening.org/index.php?module=Pagesetter&type=file&func=get&tid=5&fid=reportfile&pid=6>.
- [3] M. J. Gómez, S. Herrera, D. Solé, E. García-Calvo, A. R. Fernández-Alba. Spatio-temporal evaluation of organic contaminants and their transformation products along a river basin affected by urban, agricultural and industrial pollution. *Sci. Total Environ.* **2012**, *420*, 134.
- [4] M. J. Gómez, S. Herrera, D. Solé, E. García-Calvo, A. R. Fernández-Alba. Automatic searching and evaluation of priority and emerging contaminants in wastewater and river water by stir bar sorptive extraction followed by comprehensive two-dimensional gas chromatography-time-of-flight mass spectrometry. *Anal. Chem.* **2011**, *83*, 2638.
- [5] R. H. M. M. Schreurs, M. E. Quaedackers, W. Seinen, B. Van der Burg. Transcriptional activation of estrogen receptor ER α and ER β by polycyclic musks is cell type dependent. *Toxicol. Appl. Pharm.* **2002**, *183*, 1.
- [6] R. H. M. M. Schreurs, J. Legler, E. Artola-Garicano, T. L. Sinnige, P. H. Lanser, W. Seinen, B. van der Burg. *In vitro* and *in vivo* antiestrogenic effects of polycyclic musks in zebrafish. *Environ. Sci. Technol.* **2004**, *38*, 997.

- [7] M. Breitholtz, L. Wollenberger L. Dinan. Effects of four synthetic musks on the life cycle of the harpacticoid copepod *Nitocra spinipes*. *Aquat. Toxicol.* **2003**, *63*, 103.
- [8] L. Wollenberger, M. Breitholtz, K. Ole Kusk, B.-E. Bengtsson. Inhibition of larval development of the marine copepod *Acartia tonsa* by four synthetic musk substances. *Sci. Total Environ.* **2003**, *305*, 53.
- [9] S. Franke, C. Meyer, N. Heinzel, R. Gatermann, H. Hühnerfuss, G. Rimkus, W. A. König, W. Francke. Enantiomeric composition of the polycyclic musks HHCB and AHTN in different aquatic species. *Chirality* **1999**, *11*, 795.
- [10] SWECO Environment Screening Report. Screening of musk substances and metabolites. **2010**. Available: <http://www3.ivl.se/miljo/projekt/dvss/pdf/Muskammen2009.pdf>.
- [11] R. Gatermann, S. Biselli, H. Hühnerfuss, G. G. Rimkus, S. Franke, M. Hecker, R. Kallenborn, L. Karbe, W. A. König. Synthetic musks in the environment. Part 2: Enantioselective transformation of the polycyclic musk fragrances HHCB, AHTN, AHDI, and ATII in freshwater fish. *Arch. Environ. Contam. Toxicol.* **2002**, *42*, 447.
- [12] K. Bester. Analysis of musk fragrances in environmental samples. *J. Chromatogr. A* **2009**, *1216*, 470.
- [13] S. Biselli, R. Gatermann, R. Kallenborn, L. Sydnes, H. Hühnerfuss. *Series Anthropogenic Compounds*, (Ed: G. Rimkus). Springer, Heidelberg, Berlin, **2004**.
- [14] V. Matamoros, E. Jover, J. Bayona. Advances in the determination of degradation intermediates of personal care products in environmental matrixes: a review. *Anal. Bioanal. Chem.* **2009**, *393*, 847.
- [15] T. Cserháti. *Chromatography of Aroma Compounds and Fragrance*. Springer, Heidelberg, Berlin, **2010**.
- [16] S. W. Smith. Chiral toxicology: It's the same thing, only different. *Toxicol. Sci.* **2009**, *110*, 4.
- [17] M. D. Hernando, A. Agüera, A. R. Fernández-Alba. LC-MS analysis and environmental risk of lipid regulators. *Anal. Bioanal. Chem.* **2007**, *387*, 1269.
- [18] U.S. Environmental Protection Agency (EPA). Persistent Bioaccumulative and Toxic (PBT) Chemical Program. Available: <http://www.epa.gov/pbt/>.
- [19] J. Santiago-Morales, M. J. Gómez, S. Herrera, A. R. Fernández-Alba, E. García-Calvo, R. Rosal. Oxidative and photochemical processes for the removal of galaxolide and tonalide from wastewater. *Water Res.* **2012**, *46*, 4435.
- [20] Summary Risk Assessment Report of HHCB by The Netherlands Organization for Applied Scientific Research (TNO) and the National Institute of Public Health and the Environment (RIVM), **2008**. Available: http://esis.jrc.ec.europa.eu/doc/risk_assessment/SUMMARY/hhcbsum414.pdf.
- [21] X. Chen, U. Pauly, S. Rehfus, K. Bester. Personal care compounds in a reed bed sludge treatment system. *Chemosphere* **2009**, *76*, 1094.
- [22] P. Calza, V. A. Sakkas, C. Medana, M. A. Islam, E. Raso, K. Panagiotou, T. Albanis. Efficiency of TiO₂ photocatalytic degradation of HHCB (1,3,4,6,7,8-hexahydro-4,6,6,7,8,8-hexamethylcyclopenta[γ]-2-benzopyran) in natural aqueous solutions by nested experimental design and mechanism of degradation. *Appl. Catal. B: Environ.* **2010**, *99*, 314.
- [23] E. Eljarrat, P. Guerra, D. Barceló. Enantiomeric determination of chiral persistent organic pollutants and their metabolites. *Trends Anal. Chem.* **2008**, *27*, 847.
- [24] H. Hühnerfuss, S. Biselli, R. Gatermann, R. Kallenborn, G. G. Rimkus. Enantioselective analysis of the HHCB metabolite HHCB-lactone in environmental samples. Transport and fate. *Organohalogen Compd.* **2001**, *52*, 441.
- [25] J. D. Berset, T. Kupper, R. Etter, J. Tarradellas. Considerations about the enantioselective transformation of polycyclic musks in wastewater, treated wastewater and sewage sludge and analysis of their fate in a sequencing batch reactor plant. *Chemosphere* **2004**, *57*, 987.
- [26] K. Bester. Chirality as indications for biodegradation of the polycyclic musk fragrances AHTN and HHCB as well as the metabolite HHCB-lactone in a large-scale sewage plant as well as surface water. *Organohalogen Compd.* **2003**, *62*, 277.
- [27] C. Martin, M. Moeder, X. Daniel, G. Krauss, D. Schlosser. Biotransformation of the polycyclic musks HHCB and AHTN and metabolite formation by fungi occurring in freshwater environments. *Environ. Sci. Technol.* **2007**, *41*, 5395.